AN IMPROVED LOWER LEG MULTIBODY MODEL

H.J. Cappon, A.J. van den Kroonenberg, R. Happee, J.S.H.M. Wismans
TNO automotive, Crash Safety Centre, the Netherlands

ABSTRACT

Injuries to the lower extremities are among the most serious, non life threatening injuries occuring nowadays. In order to investigate and predict the occurrence of injuries, biofidelic research tools, like mathematical human body models are needed. The model of the lower extremity, presented here, includes active musculature, simulating bracing and fracture at certain injury thresholds found in literature. The model was validated with toe and heel impact tests on human specimens and volunteers and generally good agreement was found between experimental results and simulations. Using the model in a footwell intrusion simulation illustrates the prediction of fracture due to the contribution of active musculature in tibia loading.

LOWER LIMB INJURIES account for 37 % of the injuries sustained in car crashes, while 49 % of these injuries involve the lower leg, foot and ankle (Pattimore, 1991). Lestina (1998) found that ankle and foot injuries accounted for about one third of the lower extremity injuries. Therefore modelling of the human lower extremity has become increasingly important for studying injuries in this body region and prediction of lower extremity kinematics during a crash.

During the past years, finite element models have been developed by for instance Beaugonin (1996), Tannous (1996) and Wykowski (1998). Parenteau (1996) and Hall (1998) have developed multibody models of the lower leg, focusing on the kinematics of the ankle joint in particular.

The aim of this study was to develop a multibody model of the lower extremity, to study the influence of footwell intrusion on foot, ankle and lower leg kinematics and loads. Footwell intrusion causes dorsiflexion and in- or eversion of the foot. This study focused on dorsiflexion in particular.

Since a car occupant tends to brace before a frontal crash, the model also needed to address active musculature. An additional capability presented, is the failure occuring in tibia and ankle at specified injury thresholds.

In order to validate the model, the responses to heel and toe pedulum impacts, measured in experiments with cadaver specimens and volunteers, were compared with corresponding numerical simulations. Once the model was validated it was used to simulate lower leg responses during footwell intrusion.

METHODS

THE BASIC MODEL - Hall (1998) developed a multibody model of the human lower extremity, including thigh, leg, ankle and foot. The model was validated only for plantar impact, involving small foot rotations. The in- and eversion movement has also been incorporated, but not validated.

The hip joint, femur and knee joint were adopted from a Hybrid III database model and the pelvis was rigidly supported. The model of the leg consisted of 16 bodies, resulting in 7 rigid structures, 6 joints, 11 ligaments and 2 muscles. The joints modelled were the proximal tibia-fibular joint, the ankle joint, the subtalar joint, the tarsal joint, the metatarsal joint and the toe joint. The gastrocnemius and soleus muscle were represented by non-linear spring elements, while the most important ligaments were modelled with two parallel structures: a non-linear spring element and a Maxwell element. Thus the characteristics of the foot and ankle were partly lumped in the joint characteristics and partly modelled as separate structures, that is ligaments and muscles. The geometry of the lower leg and foot was respresented by 13 ellipsoids, as the contact areas of the foot, being the heel and the ball of the foot, can be adequately modelled with ellipsoids.

Figure 1 – Model of the lower extremity including (active) musculature shown right

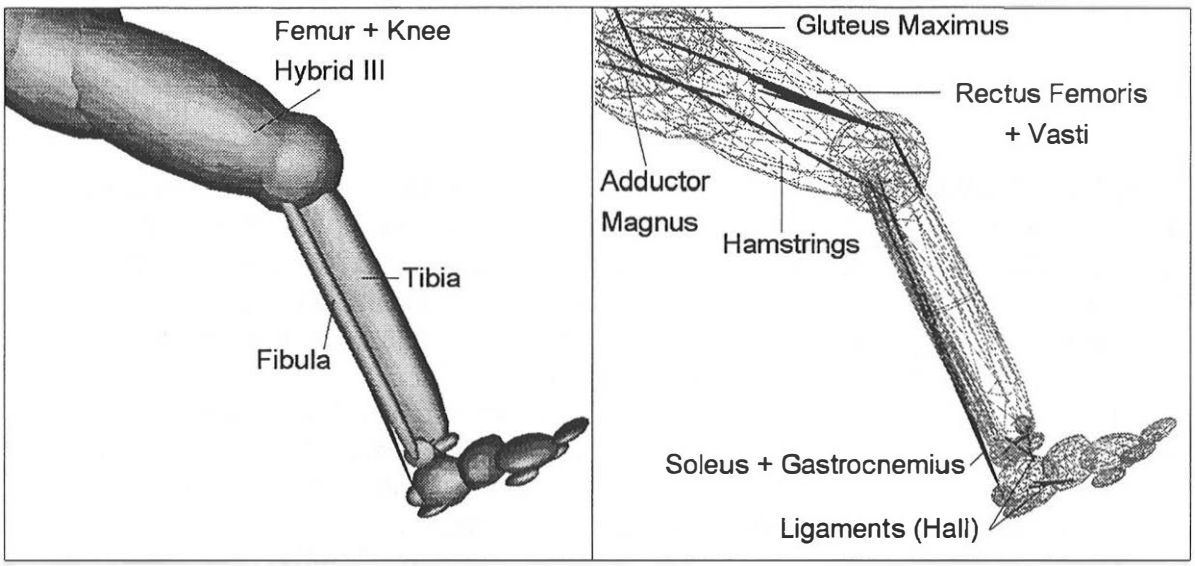

The model used in this study is a modified version of the model presented by Hall. This model extends to simulation of dorsiflexion loading as described below.

MUSCULATURE - During bracing in frontal impacts, the car occupant presses the foot against the brake pedal as was found in driving simulations performed by Owen (1998) and Palmertz (1998). The muscles mainly involved in this action are the knee extensors, the hip extensors and the ankle plantar flexors. The most important knee extensor is the quadriceps muscle in the thigh, which is attached to the patella and extends to the anterior side of the tibia. It consists of the rectus femoris and three vasti. The muscles mainly involved in hips extension are the adductor magnus, the hamstrings* and the gluteus maximus, while ankle plantar

* Biceps femoris, semitendinosus and semimembranosus

flexion is induced by the gastrocnemius and the soleus muscle, both attached to the achilles tendon (Figure 1). The insertion point of the muscles modelled were derived from Seireg (1989).

Active musculature - In MADYMO muscles can be implemented according to the model of Hill (Winters, 1990). This muscle model allows the user to specify active and passive muscle characteristics. The parameters for the active characteristics that were used in this model are presented in Appendix A, table 1. The level of activation is dependent on the application of the model.

Passive musculature - The passive behaviour of the hip and thigh muscles was based on the standard functions provided in MADYMO, while the behaviour of the lower leg muscles was adapted from Hall's model, showing stiffer functions than MADYMO.

FRACTURE - Two structures within the lower leg model were given the possibility to break: the ankle joint and the tibia. In the ankle joint a dorsiflexion angle of 45 degrees (Begeman, 1990 and Portier, 1997) or a lower tibia torque of 60 Nm (Portier, 1997) had to be exceeded for at least 1ms for the joint to break. At failure the ankle joint was removed, which meant that the ankle was attached to the foot by ligaments only after failure. The tibia failed when the axial compression force in the tibia exceeded 7.8 kN for longer than 1ms. For this purpose a translational joint was modelled in the tibia, which was locked until failure. After failure the tibia was able to translate for a few millimeters, since crush of cartilage and fracture of the tibia might involve some axial displacement of the ankle with respect to the knee. Yoganandan (1996) proposed 8.0 kN for failure, Kitagawa (1998) found 7.3 kN for pylon fractures, 8.1 kN for calcaneal fractures and reported 7.8 kN for tibial fracture found by Begeman. Figure 2 shows an example of failure on the compressive force calculated in the tibia.

Figure 2 - tibia compression force with and without failure

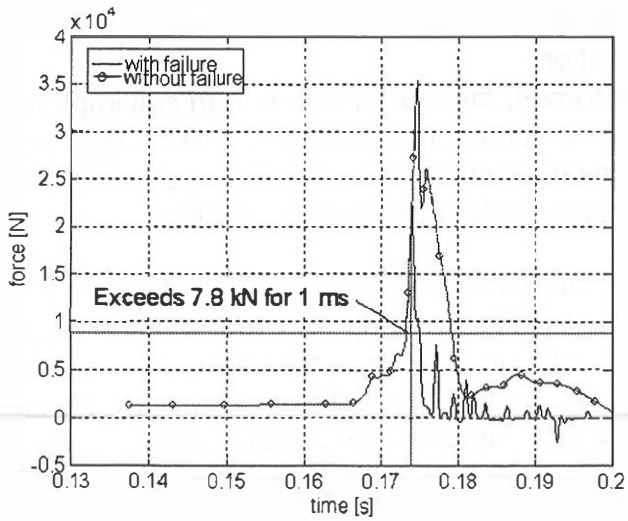

VALIDATION

At the Transport Research Laboratory (TRL) a set of toe and heel impact experiments were performed (Manning, 1998). The test were conducted using 7 human post mortem specimens and 5 volunteers. The PMHS legs were rigidly supported at the knee, while for the volunteers the knee was flexed at 90° and support was provided behind the knee. The volunteer tests were divided in aware and unaware volunteer experiments in order to evaluate muscle tension influence on the response. The setup as used at TRL was modelled and used for validation of the lower leg part of the model (Figure 3). The feet were hit with an impactor of 1.4 kg effective mass. The knee in the model was fixed, which means that only the ankle plantar flexors modelled were of influence on the response.

Figure 3– simulation of the TRL tests (fixed knee)

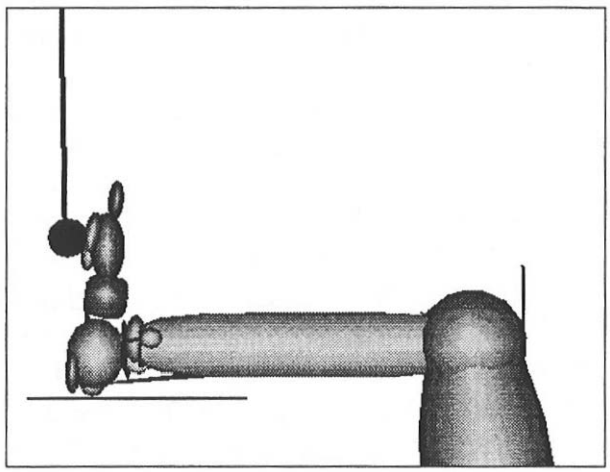

The following output parameters were compared to the test results:

1. foot rotation: the angle between the tibia and the foot (plantar flexion is +), which was measured in the volunteer experiments by means of a goniometer and checked using film data analysis;
2. pendulum acceleration;
3. tibia compressive forces, measured with a load cell implemented in the tibia of the post mortem specimen (no data available for volunteer tests);
4. tibia forward / rearward bending torque, measured with the tibia load cell mentioned (no data available for volunteer tests).

The PMHS tests were simulated using passive muscles, thus assuming comparable tensile characteristics for living and post mortem muscle tissue. This is a usual approach, although some difference has been reported (Ee et al, 1998).

The responses of unaware volunteer tests were compared with simulations involving passive musculature, although the muscle activity of unaware volunteers was not completely negligible. The aware volunteer experiments were compared with the simulations involving active musculature (Table 1) using a muscle activation level of 30 %.

Table 1 – Matrix of validations applied

	PMHS specimen	Volunteer unaware (passive)	Volunteer aware (active)
Toe impact 2 m/s		x	x
Toe impact 4 m/s	x	x	x
Heel impact 2 m/s	x		
Heel impact 4 m/s	x		

RESULTS

TOE IMPACT – Mainly the results of the 4 m/s simulations will be shown in this paragraph. Additional figures are shown in appendix B.

The simulation of the impact at the ball of the foot (active muscles) showed that the foot initially dorsiflexes. Plantar flexion follows after 60 ms, which is less clear in the (aware) volunteer tests (Figure 4). This phenomenon can be fully attributed to the muscles that are activated 30 % throughout the entire simulation (activation starting at t=0 s).

Figure 4 - foot rotation, ball impact at 4 m/s; active muscles

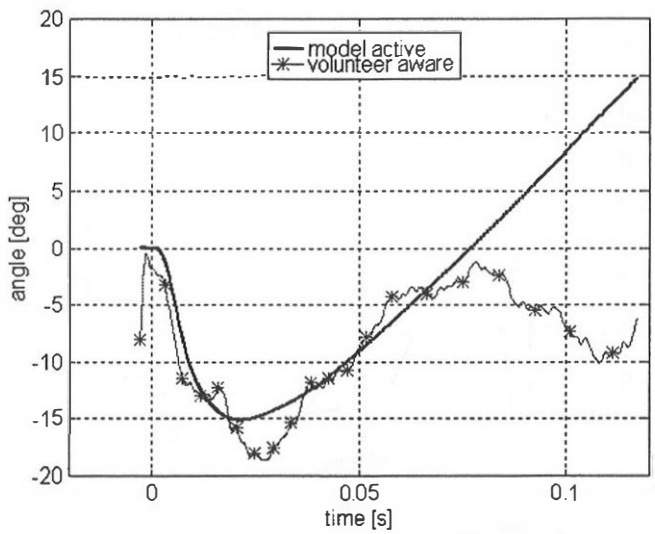

The foot rotation data of unaware volunteer tests, at 4 m/s ball impact, showed very large variations (Appendix B) and were not suitable for validation purposes. The simulation at 2 m/s, on the other hand, showed good results (Figure 5).

The forces calculated in the tibia are generally close to the measured values in the PMHS specimen (Figure 6). The main difference is that the force curve in the specimen tests lasts longer than in the simulation, which can partly be explained by the foot contact stiffness used (see below).

The torques in the tibia calculated at toe impact were much too high (Figure 7). It was found that the applied rotational damping of the foot ankle complex, which is lumped in the ankle joint, was the cause of this discrepancy. Decreasing the damping caused lower tibia torques as can be seen in Figure 7. This parameter was adopted from the original model (Hall, 1998) and seems to be chosen arbitrarily. The damping of the ankle apparently needs further study.

Figure 5 – foot rotation, ball impact at 2 m/s; passive muscles

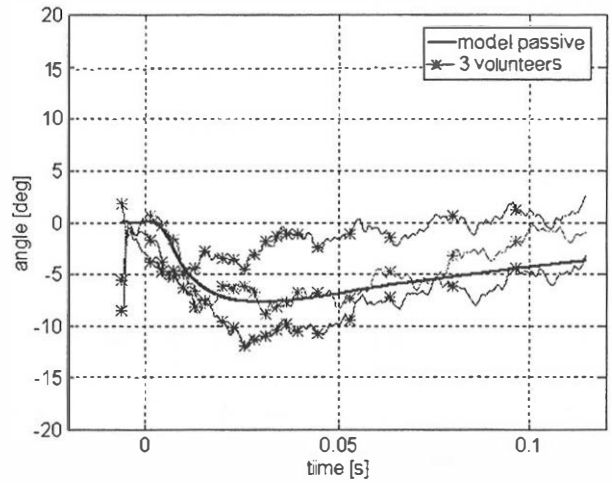

Figure 6 - tibia compressive force, ball impact at 4 m/s; passive muscles

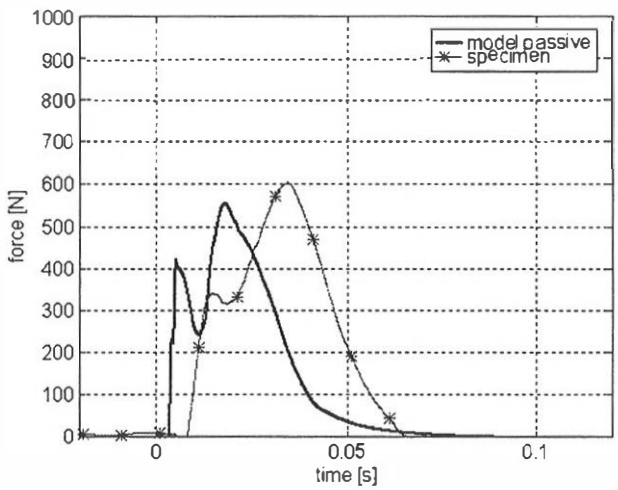

The magnitude of the calculated pendulum accelerations were found to be very close to the experimental results in all ball impact simulations, but the duration of the acceleration was generally too short. A possible cause of this shorter duration is that the rubber shoe representation, used in the experiments, was not modelled. The shoe was omitted in the simulation, because the responses were found to be relatively insensitive to changes in damping an stiffness in the contact interaction between foot and impactor. Only the time range of the tibia force and of the acceleration peak increased due to a decreasing foot stiffness.

Figure 7 - tibia torque, ball impact at 4 m/s; passive muscles

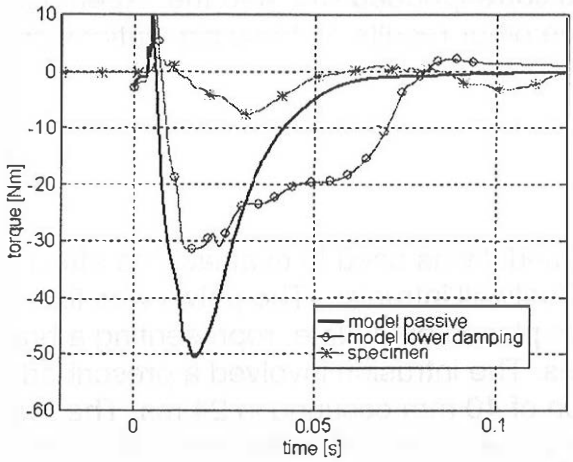

Figure 8 - pendulum acceleration, ball impact at 4 m/s; passive muscles

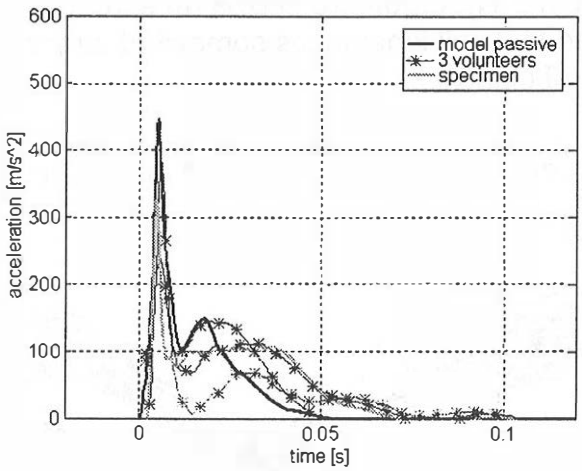

Figure 9 - tibia compressive forces, heel impact at 2 m/s

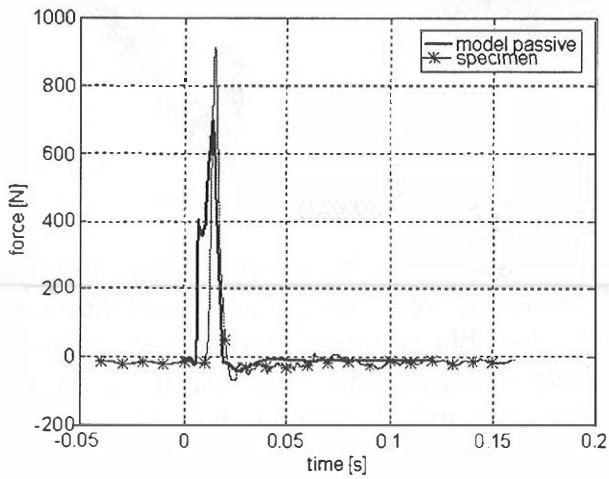

HEEL IMPACT - As the loading path to the tibia is much shorter than for the toe impact, these responses corresponded well with the experimental data. Figure 9 shows the tibia force. The other results of these simulations can be found in appendix B.

APPLICATION

Finally the lower leg model was used to evaluate the effect of muscle activity on the response in case of footwell intrusion. The pelvis was fixed, while the ball of the foot of the model was placed on a plate, representing a brake pedal, with an initial angle of 60 degrees. The intrusion involved a prescribed rotation of 15 degrees and a translation of 40 mm occuring in 24 ms. The brake pedal could not be depressed, since the influence on the loads in the tibia and rotations of the foot, was found to be small (Rudd, 1998). The normal force acting on the brake pedal was set to 800 N, as was approximately found by Owen (1998) and Palmertz (1998), which means a muscle activation level of 30 % in this model (shear forces on the pedal were below 150 N). Figure 10 shows an example of an intrusion sequence with prescribed footwell kinematics somewhat larger than mentioned above, only for the sake of clarity.

Figure 10 – Footwell intrusion, 30° rotation and 80 mm displacement in 24 ms

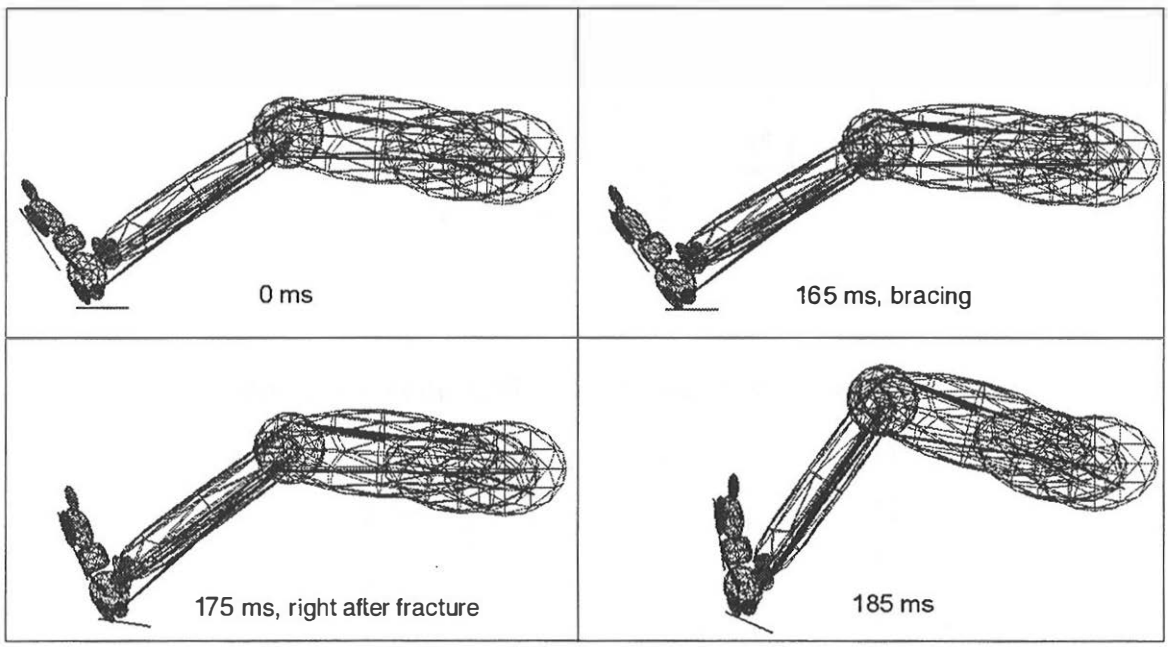

It was found that the fracture in the tibia occured due to the activated muscles, as the tension in the achilles tendon causes an additional increase in the tibia loading. Figure 11 presents the tibia compressive force for active and passive muscle behaviour. The active muscles cause the tibia to break, while the tibia stays intact with passive muscles. In both simulations the ankle breaks due to the large tibia torque, at 0.328 seconds in the active simulation and at 0.335 seconds in the passive simulation.

Figure 11 - tibia compressive force during footwell intrusion. Active and passive

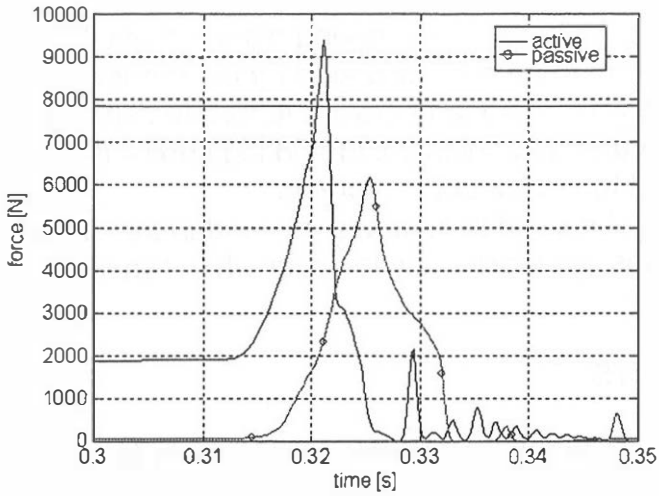

DISCUSSION

A multibody model has been presented, which is capable of predicting foot and ankle kinematics in a crash involving footwell displacement and rotation. The influence of active musculature on tibia loads and lower leg kinematics has been evaluated and fracture has also been modelled. The model was validated with experimental data involving toe and heel impacts on a PMHS specimen and 3 volunteers. The rotation of the foot and the compressive loads in the tibia were predicted very well by the model and therefore injury prediction based on these parameters is very well possible.

The mayor improvement of the current model with respect to Hall's model is that active musculature has been added. Furthermore the active musculature enables the user to simulate the effect of bracing during a crash. Petit (1998) studied the effect of active musculature on a Hybrid III dummy model and found significant changes in the response due to active muscles, as was found here. Modelling of fracture clearly showed that the chance of fracture increased with increasing muscle activity, as it caused an increasing tibia compression force. A limitation of modelling fracture, is that prediction of kinematics after failure is not possible in this case, due to the dependency on the modification in the internal structure. Furthermore, prediction of fracture sequence is thus questionable as well. Note that, as soon as an injury threshold is exceeded, the kinematic behaviour of the model without fracture, is questionable as well. The validation and application of the model only considered dorsiflexion and translation of the foot, as this is generally occuring during footwell intrusion. In order to make the model more widely applicable, it is recommended to validate the model with in- and eversion impact experiments. In the near future the leg model will be included in the human body model as presented by Happee (1998).

CONCLUSIONS

- The model of the human lower extremity presented is able to predict tibia compressive forces and foot rotation during plantar impact of the foot.
- The tibia torques seem to be overestimated by the model, but decreasing the ankle joint damping was found to improve the torque considerably.
- The active musculature in the hips, thigh and leg shows the capability of modelling bracing of the occupant in a crash.
- Bracing during impact proved to increase the load in the tibia considerably and showed that fractures are more likely to occur when bracing.

ACKNOWLEDGEMENTS

The authors would like to thank the University of Virginia for providing the initial model, which was partly developed in collaboration with TNO. Furthermore, special thanks to Lucy Wheeler and Clare Owen at Transport Research Laboratory, for providing the experimental data.
Part of this study was financed by the European ADRIA project (PL96-1074)

REFERENCES

1. Begeman, P.C., Prasad, P. Human Ankle Impact Response in Dorsiflexion. SAE has also been modelled. The model was validated with 902308 (1990).
2. Beaugonin, M., Haug, E., Cesari, D. A Numerical Model of the Human Ankle/Foot under Impact Loading in Inversion and Eversion. SAE 962428 (1996).
3. Brand, R.A., Pedersen, D.R., Friederich, J.A. The Sensitivity of Muscle Force Predictions to Changes in Physiologic Cross-Sectional Area. In Journal of Biomechanics Vol. 19 No. 8 (1986) pp. 589-596.
4. Van Ee, C.A., Chasse, A.L., Myers, B.S. The Effect of Postmortem Time and Freezer Storage on the Mechanical Properties of Skeletal Muscle. SAE 983155 (1998).
5. Hall, G.W. Biomechanical Characterization and Multibody Modeling of the Human Lower Extremity. PhD Dissertation, University of Virginia (1998).
6. Hall, G.W., Crandall, J.R., Pilkey, W.D., Thunnissen, J.G. Development of a dynamic multibody model to analyze human lower extremity impact response and injury. IRCOBI proceedings 1998.
7. Happee, R., Hoofman, M., Kroonenberg, A.J. van den, Morsink, P., Wismans, J. A Mathematical Human Body Model for Frontal and Rearward Seated Automotive Impact Loading. SAE 983150 (1998).
8. Kitagawa, Y., Ichikawa, H., Pal, C., King, A.I., Levine, R.S. Lower Leg Injuries Caused by Dynamic Axial Loading and Muscle Tensing. ESV 98-S7-O-09. (1998).
9. Lestina, D.C., Kuhlmann, T.P., Keats, T.E., Alley, R.M. Mechanisms of Fracture in Ankle and Foot Injuries to Drivers in Motor Vehicle Crashes. SAE 922515 (1992).
10. Manning, P., Owen, C., Roberts, A., Oakley, C., Lowne, R., Wallace, A. Dynamic Response and Injury Mechanism in the Human Foot and Ankle and an Analysis of Dummy Biofidelity. ESV 98-S9-O-11 (1998).
11. Owen, C., Roberts, A., Manning, P., Lowne, R. Positioning and Bracing of the Lower Leg during Emergency Braking - a Volunteer Study. IRCOBI proceedings 1998.

12. Palmertz, C., Jakobsson, L., Karlsson, A. Pedal Use and Foot Positioning during Emergency Braking. IRCOBI proceedings 1998.
13. Parenteau, C.S. Foot-Ankle Joint Responses, Epidemiology, Biomechanics and Mathematical Modeling. PhD Dissertation, Chalmers University of Technology (1996).
14. Pattimore, D., Ward, E., Thomas, P., Bradford, M. The Nature and Cause of Lower Limb Injuries in Car Crashes. SAE 912901 (1991).
15. Petit, Ph., Portier, L., Trosseille, X. Rigid Body Model of the Hybrid III Dummy Lower Limb Including Muscle Tension under Car Crash Conditions. IRCOBI proceedings 1998.
16. Portier, L. Petit, Ph., Dômont, A. Trosseille, X., Le Coz, J., Tarrière C., Lassau, J. Dynamic Biomechanical Dorsiflexion Responses and Tolerances of the Ankle Joint Complex. SAE 973330 (1997).
17. Rudd, R.W., Sieveka, E.M., Crandall, J.R., Pellettiere, J., Lynn, S., Keller, J. Lower Extremity and Brake Pedal Interaction in Frontal Collisions: Computer Simulation. SAE 980364 (1998).
18. Seireg, A., Arvikar, R. Biomechanical Analysis of the Musculoskeletal Structure for Medicine and Sports (1989).
19. Tannous, R.E., Bandak, F.A., Toridis, T.G., Eppinger, R.H. A Three-Dimensional Finite Element Model of the Human Ankle: Development and Preliminary Application to Axial Impulsive Loading. SAE 962427 (1996).
20. TNO Crash-Safety Research Centre. Theory Manual 3D and User's Manual 3D of MADYMO version 5.3 (1997).
21. Winters, J.M., Stark, L. Estimated Mechanical Properties of Synergistic Muscles Involved in Movements of a Variety of Human Joints. In Journal of Biomechanics Vol. 21 No. 12 (1988) pp. 1027-1041.
22. Winters, J.M., Woo S.L-Y. Hill-based muscle models: A systems engineering perspective. In Multiple Muscle Systems: Biomechanics and Movement Organization (1990) pp 69-93.
23. Wykowski, E., Sinnhuber, R., Appel, H. Finite Element Model of Human Lower Extremities in a Frontal Impact. IRCOBI proceedings 1998.
24. Yoganandan, N., Pintar, F.A., Boynton, M., Begeman, P., Prasad, P., Kuppa, S.M., Morgan, R.M., Eppinger, R.H. Dynamic Axial Tolerance of the Human Foot-Ankle Complex. SAE 962426 (1996).

APPENDIX A

Muscle parameters - These values were calculated according to Winters (1988), with Vmax=5 x L0 and Fmax=0.5 x PCSA (with PCSA in m^2). No activation and exitation time constants were found for the Gluteus Maximus and the Adductor Magnus. These values were copied from the Hamstrings. Values that are not mentioned in the table have been set to MADYMO default (see MADYMO User's Manual 3D).

Table 1 - Muscle parameters

Muscle	PCSA [cm^2]	Ta [ms]	Tn [ms]	L0 [m]	Vmax [m/s]
Rectus Femoris	20	9	30	0.37	1.88
Vastus Lat.	40	16	39	0.20	0.98
Vastus Int.	25	13	34	0.19	0.95
Vastus Med.	30	17	37	0.21	1.05
Gastroc. Med.	20	11	31	0.46	2.30
Gastroc. Lat.	12	9	29	0.46	2.28
Soleus	40	31	43	0.35	1.78
Gluteus Maximus	40	17	34	0.18	0.87
Hamstrings	46	17	34	0.46	2.20
Adductor Magnus	40	17	34	0.19	0.90

abbreviations of table 1: PCSA = Physiological Cross-Sectional Area; Ta = activation time constant; Tn = excitation time constant; L0 = rest length of the muscle; Fmax=maximum muscle force; Vmax = maximum contraction velocity;

Petit (1998) used values for Vmax, which differed up to one order of magnitude with the ones presented here. He also used different values for Fmax. The responses, however, calculated with the values according to Petit, differed little from the responses calculated here.

APPENDIX B

This appendix contains all remaining figures of the validation of the model. The figures below contain pendulum accelerations, foot rotation angles, tibia y-torques and tibia compressive forces. Each set of figures contains a header with the test conditions.

Active musculature, ball impact at 2 m/s

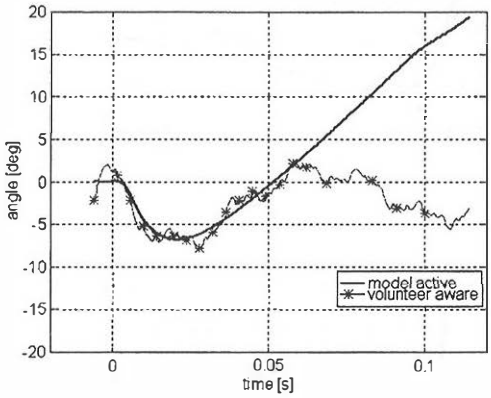

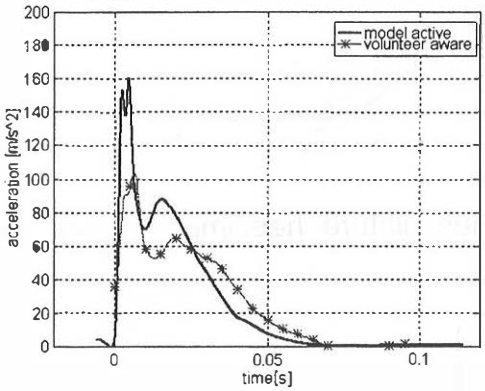

Passive musculature, ball impact at 2 m/s

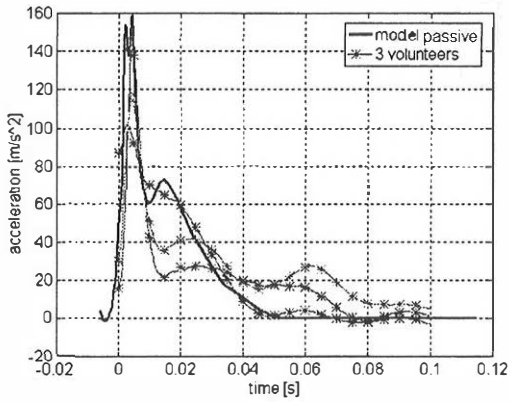

Passive musculature, heel impact at 2 m/s

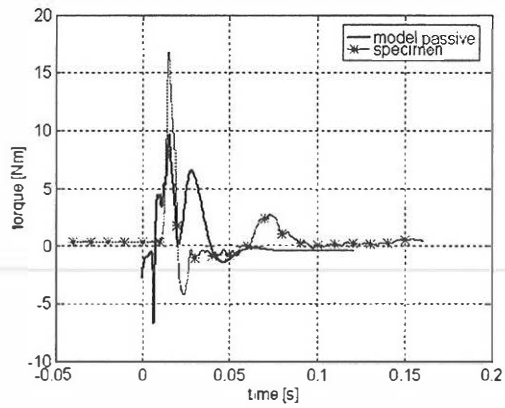

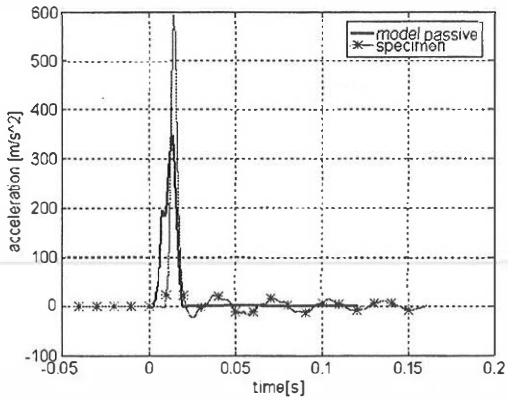

Active musculature, ball impact 4 m/s

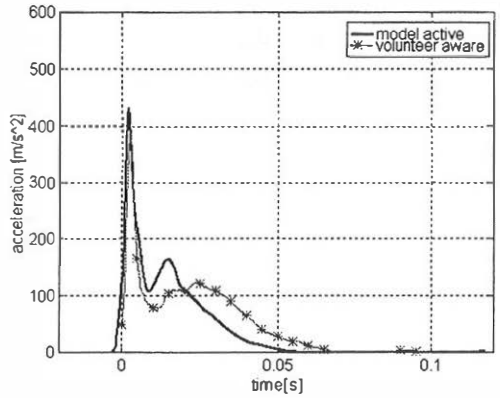

Passive musculature, ball impact 4 m/s

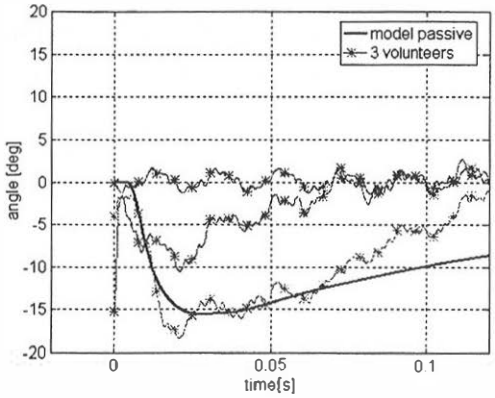

Passive musculature, heel impact 4 m/s